




3D Imaging of southernmost Triassic archosaur footprints from Europe (Southern Spain)

Jesús Reolid¹  · F. Javier Cardenal² · Matías Reolid³ · Emilio Mata²

Received: 20 December 2019 / Accepted: 15 April 2020 / Published online: 5 May 2020
© Universidad Complutense de Madrid 2020

Abstract

The application of 3D photogrammetric models to the analysis of raurisuchian archosaur footprints of the Middle-Upper Triassic of the south Iberian palaeomargin improves the knowledge and interpretation of the behaviour of raurisuchian archosaurs that inhabited this area. Two outcrops rich in footprints were scanned at Santisteban del Puerto and Cambil in Jaén (SE Spain). The footprints of Santisteban del Puerto consist of three subparallel concave impressions including two long lateral traces, and a shorter medial one. The footprints of Cambil are preserved as convex hyporeliefs, counter-moulds, at the bottom of inverted strata and record manus and pes impressions. The 3D photogrammetric models provide new data sets such as depth distribution maps, contour line maps, and topographic profiles of the footprints that implement the interpretation obtained during fieldwork. These are useful tools for the study, preservation, and dissemination of such outcrops. Digitally generated depth distribution maps display darker (blue) colours for the most depressed areas of the traces. The contour line maps and digital elevation models of the footprints improve the understanding of the locomotion of the tracemaker. The footprints of Cambil and Santisteban del Puerto represent the only ichnological record of Triassic terrestrial vertebrates in the southern Iberian Peninsula, and the southernmost record of trace fossils of the Triassic in Europe. These outcrops also provide information about different locomotion styles of Triassic archosauromorphs including swimming/floating of bipeds (Santisteban del Puerto) and walking of quadrupeds (Cambil).

Keywords Vertebrate ichnology · Tabular cover · Subbetic · Photogrammetry · TLS · 3D models · Triassic

Resumen

El uso de modelos fotogramétricos 3D para el análisis de las huellas de archosaurios raurisuchianos del Triásico medio-superior del paleomargen Sudibérico amplió el conocimiento y la interpretación del comportamiento de los archosaurios raurisuchianos que habitaban esta área. Se escanearon dos afloramientos ricos en huellas en Santisteban del Puerto y Cambil en Jaén (SE España). Las huellas de Santisteban del Puerto consisten en grupos de tres impresiones cóncavas subparalelas que incluyen dos trazos laterales largos y uno medio más corto. Las huellas de Cambil se conservan como hiporelievesm convexos, contramoldes, en el fondo de estratos invertidos y registran impresiones de manus y pes. Los modelos fotogramétricos en 3D proporcionan nueva información, como modelos digitales de elevación, mapas de líneas de contorno y perfiles topográficos de las huellas que complementan la interpretación obtenida durante el trabajo de campo. Estas son herramientas útiles para el estudio, preservación y difusión de tales afloramientos. Los modelos digitales de elevación generados muestran colores más oscuros (azules) para las áreas más deprimidas de las trazas. Los mapas de líneas de contorno y los modelos digitales de elevación de las huellas mejoran la comprensión de la locomoción del trazador. Las huellas de Cambil y Santisteban del Puerto representan el único registro icnológico de vertebrados terrestres del Triásico en el sur de la Península Ibérica, y el registro más meridional de trazas fósiles del Triásico en Europa. Estos afloramientos también proporcionan información sobre los diferentes estilos de locomoción de los archosauromorfos del Triásico, incluida la natación/flotación de bípedos (Santisteban del Puerto) y caminantes cuadrúpedos (Cambil).

Electronic supplementary material The online version of this article (<https://doi.org/10.1007/s41513-020-00125-0>) contains supplementary material, which is available to authorized users.

✉ Jesús Reolid
jreolid@ugr.es

Extended author information available on the last page of the article

Palabras clave Ichnología de vertebrados · Cobertera Tabular · Subbética · Fotogrametría · TLS · Modelos 3D · Triásico

1 Introduction

Archosauromorpha is a clade that radiated during the Triassic and includes the crown group Archosauria with Pseudosuchia (crocodylan-stem) and Avemetatarsalia (dinosaur-stem) archosaurs, as well as some common ancestors (s. Nesbitt 2011). Body fossil remains of pseudosuchian archosaurs in the Iberian Plate are scarce and the record corresponds mainly to fossil footprints (see Demathieu et al. 1978; Gand et al. 2010; Fortuny et al. 2011; Díaz-Martínez et al. 2015; Mujal et al. 2015, 2016, 2017) represented by the ichnogenera *Chirotherium*, *Brachychirotherium*, *Isochirotherium* and *Synaptichnium* (see Demathieu et al. 1978; Sanz et al. 1990; Pérez-López 1993). Other Triassic trace fossils produced by swimming bipedal archosaurs have also been reported (Reolid and Reolid 2017). The makers of chirotheriid tracks were archosaurs with (1) a pentadactyl pes and manus showing a reduced postero-laterally positioned digit V, (2) pronounced heteropody and (3) narrow gait (Haubold 1971; Demathieu and Demathieu 2004; Klein and Haubold 2007).

“Rauisuchia” is an informal group (s. Nesbitt 2011) to name most of the pseudosuchians that lived during the Triassic period, mainly large archosaurs, represented by the clades Rauisuchoidea and Poposauroidea (Brusatte et al. 2010). Rauisuchoid archosaurs are the producers of some chirotheriid trace-fossils characterised by pentadactyl footprints with pronounced heteropodia and digit V located in a postero-lateral position.

Geomatic techniques are increasingly becoming standard methods for surface digitizing in Earth Sciences applications. More specifically, heritage and palaeontology has greatly benefited from these new measuring and documentation techniques. Indeed, digital three-dimensional (3D) models are revolutionizing palaeontological geometric analysis (Molnar et al. 2012; Cunningham et al. 2014; Mallison and Wings 2014; Evin et al. 2016). Among these techniques, those based on image (photogrammetry) and range (aerial and terrestrial laser scanner, ALS/TLS) data are of primary importance (Zhilin and Baltsavias 2008). They are especially adapted for the acquisition and edition of the spatial information and allow the acquisition of reliable and high-resolution 3D models of both the palaeontological samples and the context—the outcrops—where the samples are found.

3D photogrammetric models are useful for taxonomical analyses but also for ethological interpretations. The use of photogrammetry of footprints for ichnological research has been widely applied before to Triassic examples (Mujal et al. 2015, 2017; Lagnaoui et al. 2019; Marchetti et al. 2019).

The application of this technique to the analysis of archosaur footprints from the Middle-Upper Triassic of the south Iberian palaeomargin, especially in the case of the enigmatic footprints of the Tabular Cover, allows enhancement of the knowledge and interpretation of the behaviour of these reptiles in this area. Thus, the main objective of this research is the description and identification of archosaur footprints and its tracemaker’s behaviour applying photogrammetric techniques.

2 Geological setting

The studied examples correspond to the Triassic of the Tabular Cover (Santisteban del Puerto outcrop) and the Subbetic (Cambil outcrop) in the province of Jaén, SE Spain (Fig. 1). In both cases, the fossil footprints are preserved in red sandstones and siltstones (Fig. 2).

In southern Spain, the Triassic red beds of the Tabular Cover, represented by the Chiclana de Segura Formation, contain the enigmatic trace fossils from the Santisteban del Puerto outcrop (Demathieu et al. 1999; Reolid and Reolid 2017). The Tabular Cover occurs along the southeastern edge of the Iberian Variscan Massif as a belt of horizontal redbeds (Fig. 1). The Chiclana de Segura Formation is characterised by continental Triassic deposits (redbed facies) unconformably overlying the Palaeozoic basement (e.g. Simon 1987; Pérez-López 1998; Bourquin et al. 2011; López-Gómez et al. 2012). The facies are mainly continental red sandstones and siltstones, with gypsum-rich levels in the transition to the overlying Jurassic limestones (Fig. 1). The Triassic deposits of the Chiclana de Segura Formation developed in a fluvial-coastal system during the Middle to Late Triassic (Fernández 1977; Pérez-López and Pérez-Valera 2007). This formation is almost 300 m thick in the studied area (north-eastern Jaén province), and constitutes a uniform and monotonous succession whose precise stratigraphic age is difficult to determine.

To the south, the redbeds of the Tabular Cover change to Germanic Facies deposits in the Prebetic (Hornos-Siles Formation) and in the Subbetic (Majaniillos Formation and Jaén Keuper Group). Therefore, from the Tabular Cover deposited directly on the Iberian Variscan Massif to the south, carbonates of the Muschelkalk facies appear and evaporites of the Keuper facies become progressively more common (López-Garrido 1971). The fossil footprints reported by Pérez-López (1993) and the new fossil footprints come from sandstone levels of the Keuper facies near the locality of Cambil (Fig. 1).

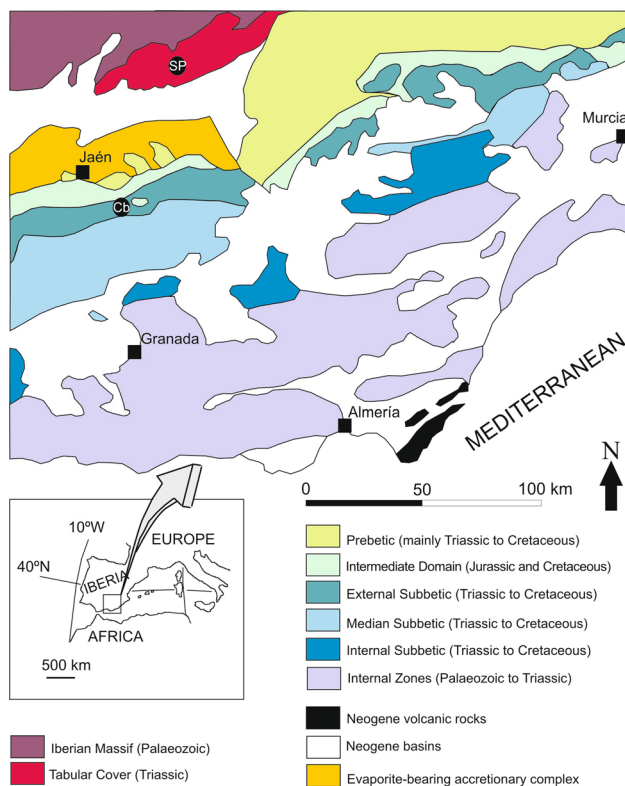


Fig. 1 Location of the study outcrops of Santisteban del Puerto (SP) in the Tabular Cover and Cambil (Cb) in the Betic Cordillera, SE Spain (detail in Fig. 2)

The Santisteban del Puerto outcrop is located in the north of the Jaén Province, close to the road A-312, 800 m west of Santisteban del Puerto village. The stratigraphic interval with the fossil footprints is constituted by Middle Triassic sandstones with cross lamination, siltstones, and limestones (Fig. 2). The footprints are located at the top of a grey to green sandstone bed (32 cm thick) with subhorizontal cross-lamination, and vertical and subhorizontal burrows (Fig. 2; Reolid and Reolid 2017). The beds above the trace fossils are red siltstone and sandy limestones with horizontal lamination, locally cross lamination, bivalve moulds, and *Rhizocorallium* trace fossils.

The fossil footprints of the Subbetic were recovered 1 km southeast of Cambil (Pérez-López 1993) and the new ones just in the south exit of the town. In both cases they are preserved in sandstone beds of the Upper Triassic Keuper facies. The stratigraphic succession is composed by red (locally green) siltstones with decametric-scale sandstone layers (Fig. 2). Most of the sandy beds present cross lamination and an erosive base. The fossil footprints recovered by Pérez-López (1993) were recorded in a sandstone bed 40-cm thick, with cross lamination. The new footprints, a total of three, are located each one in different successive sandstone beds in a dump in the outskirts of Cambil village.

3 Materials and methods

The main technique applied to analyse the archosaur footprints has been photogrammetry, although an additional terrestrial laser scanner (TLS) survey was carried out for the 3D reconstruction of the Santisteban del Puerto outcrop. Two non-metric off-the-shelf cameras were employed. The main camera was a MILC (mirrorless interchangeable lens camera) Sony ILCE-5000 (APS-C format, 20 Mpx, pixel size 4.4 μm) with two different lenses. The lenses were a wide-angle Sony E 16 mm f/2.8 fixed focal length (24 mm in equivalent 35 mm format) and a normal angle Sony E 30 mm f/3.5 fixed focal length (45 mm in equivalent 35 mm format). The second camera was a Samsung Galaxy smart camera (1/2.3" format, 12 Mpx, pixel size 1.5 μm) and a 4.1–86.1 mm zoom lens. In order to avoid errors due to the instability of this Samsung zoom lens camera, only the wide-angle end position (4.1 mm) was used. The terrestrial laser scanner was a Leica Geosystems C10 pulsed type scanner (Fig. 3). Its main technical specifications are: range of 0.1 m–300 m; scan rate up to 50,000 points/sec; and horizontal and vertical field of view up to 360° and 270°, respectively. Moreover, the accuracies of the C10 scanner are 6 mm in position and 2 mm in the modelled surface. Laser data were processed with Leica Cyclone and Maptrek™ I-Site Studio software.

Planning close range photogrammetry projects is a challenging task since they are a combination of conventional stereo-photogrammetric projects with convergent close-range networks under special constraints (reduced object size and depth of field, proper illumination, rough microtopography with frequent occluded areas, non-metric camera lenses with high distortion values and unknown precise calibration parameters, etc.). The photogrammetric working networks and the instrumentation were selected according to the different sample shapes and sizes (Fig. 3). Table 1 summarizes the different networks and instrumentation used in this work.

After data acquisition, the images blocks were adjusted with a commercial photogrammetric software Agisoft PhotoScan (Agisoft 2019). At this stage, since the cameras were not metric, they were calibrated adjusting focal length, distortion parameters, etc. This software allows the generation of dense point clouds and then a triangulation process generates a mesh, which in fact is a virtual 3D model (Fig. 3). The model can be solid or photorealistic if photo textures (from the original images) are added. Finally, digital elevation or surface models (DEM or DSM) are built, as well as orthoimages (Fig. 3). Further, these products, the 3D models, DEMs and orthoimages were processed to make the geometric analysis of the footprints. Additional free software was also used for further

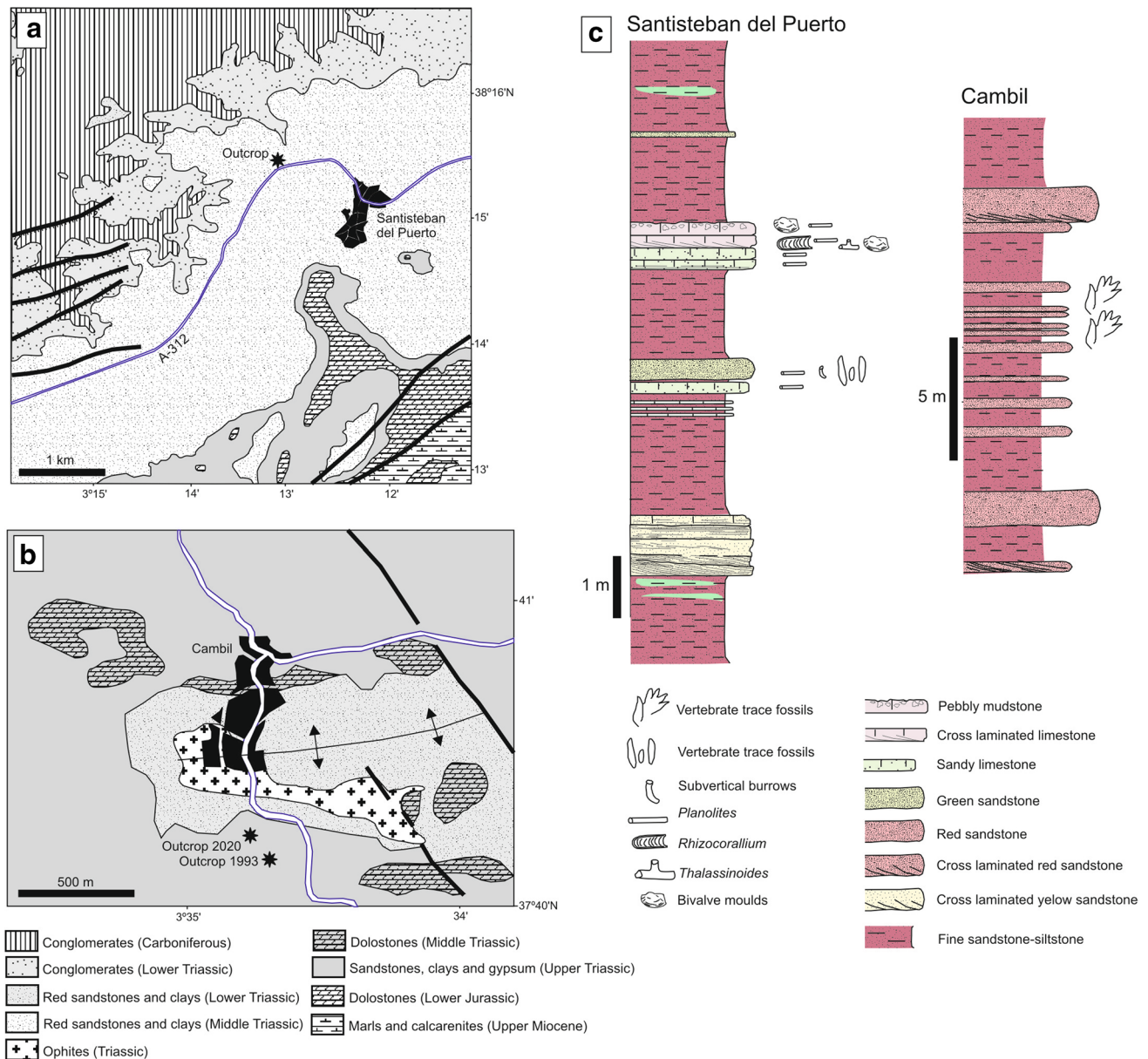


Fig. 2 Geographical position and geology of the study areas. **a** Santisteban del Puerto, and **b** Cambil. **c** Lithological column of Santisteban del Puerto (left) and Cambil (right) with sediments and sedimentary features, ichnofossils, body fossils and their position

data processing (Cloud Compare V2, for edition of point clouds and 3D models, and QGIS 3.6, for GIS processing of the orthoimages and the DEMs; CloudCompare 2019; QGIS 2019, respectively). Figure 3 shows a general workflow of the whole process.

3.1 Santisteban del Puerto footprints

The Santisteban del Puerto outcrop covers an area of approximately 18 m². Due to this size, a laser scanner survey was an effective option to make a general model of the outcrop. Five scan stations were set up to digitalise

the whole outcrop (Fig. 4). The scan density was 1 cm at 10 m, but at the area of interest (neglecting points at the walls) after merging all five scan-stations, the point cloud had 13,167,495 points, and the final resolution was near 43 points/cm² (3 points/5 mm). Despite this huge amount of data, there were not enough data at some footprints due to occlusions in the micro-topography. Therefore, in order to complete a detailed model of both the outcrop and the footprints an additional photogrammetric survey at close range was carried out.

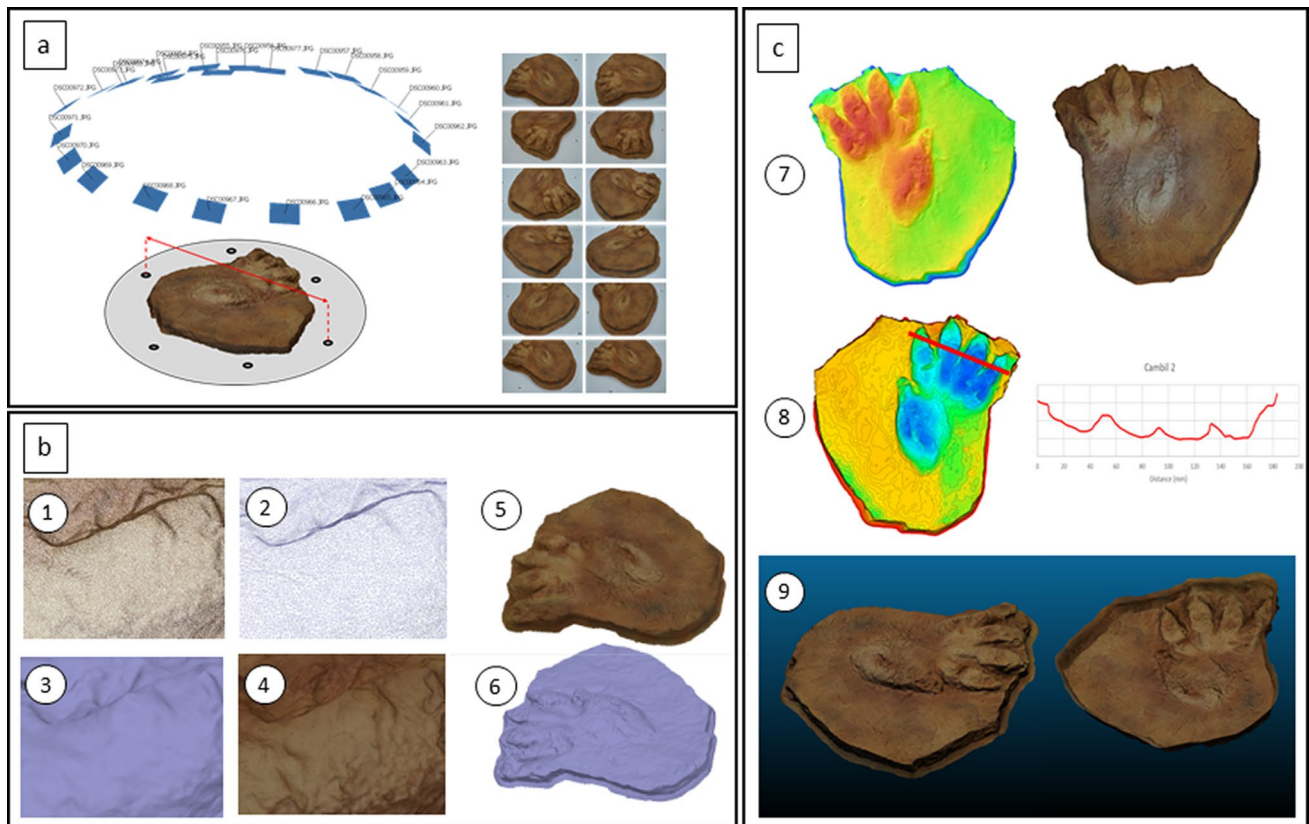


Fig. 3 Methodology workflow. **a** Data acquisition and image block alignment, including camera poses and calibration calculations, control point marking and scale adjustment. **b** (1) Dense point cloud; (2) triangulated wireframe; (3) solid mesh; (4) photorealistic textures are added; and 3D model generation (5, photorealistic; 6, solid).

c Product generation and geometric analysis: (7) digital elevation models and orthoimages; (8) Geometric analysis: depth inversions, profiles, measurements, etc.; (9) generation of virtual 3D models (obj, wrml, pdf 3D,...) for visualization, dissemination, analysis, conservation, etc.

Table 1 Summary of different networks and instrumentation used in this work

Outcrop	ID	Camera/lens scanner	No. of images	Mean distance (cm)	Mean GSD (mm)	pixel error	Approx. sample size (cm)	No. of 3D points
Cambil	Pd ₁ and Md ₁	Sony ILCE-5000 30 mm	67	60.7	0.08	0.39	68×37	2,731,717
	Pz ₂		35	56.1	0.07	0.52	36×35	3,238,465
	Pz ₁		60	38.3	0.05	0.44	24×24	1,551,204
	1B	Samsung Smart camera 4.1 mm	48	99.2	0.31	1.19	28×30	607,232
	2B		22	68.9	0.22	1.12	35×24	1,165,566
Santisteban del Puerto	General	Sony ILCE-5000 16 mm Laser scanner Leica C10	189	190	0.51	1.27	554×556	15274037 ^a
	H5	Sony ILCE-5000 16 mm					38×33	564,863
	H1						35×36	170,587
	H6						27×33	113,829
	H9						39×35	296,400

ID of the Cambil footprints after Pérez-López (1993). ID of the Santisteban del Puerto footprints after Reolid and Reolid (2017)

^aMerged point cloud (laser and photogrammetric 3D points)

This photogrammetric network consisted in 189 overlapping oblique images following several parallel and cross lines (Fig. 5). Some images were taken at very close range to avoid occluded areas at some footprints, mainly those with deeper relief. The images were registered by measuring some identifiable natural points in both the laser point cloud and the images, so both datasets were in the same coordinate reference system. The resulting photogrammetric point cloud (2,106,542 points) was generated and merged with the laser point cloud (Fig. 6; Table 1). Some of these photographs were processed again in order to generate higher density point clouds at some footprints (samples H1, H5, H6, and H9; Table 1).

3.2 Cambil footprints

The first samples of Cambil footprints (Pd_1 and Md_1 , Pz_2 , and Pz_1 ; Table 1) are those described in Pérez-López (1993). Although a previous 3D digitalization of the original manus and pes footprints had been carried out with an analytical stereoplotter and film-based images (Cardenal et al. 2001), new more detailed 3D models have been obtained with the new methods and instruments. In this case, high-fidelity polyurethane-resin cast copies were used for digitalization since the original samples are now exposed in the Parque de las Ciencias Museum of Granada (Spain).

The other two Cambil samples (Pz_2 and Pz_1 ; Table 1) were single footprints. In these cases, the sample size allowed the use of an automatic turntable so high overlapping images were taken each 5° – 10° intervals (Fig. 3). Tape measurements between coded targets allowed scaling the

models. The Cambil Pd_1 and Md_1 footprints were together in a single plate. The size of the plate is $68\text{ cm} \times 37\text{ cm}$. The plate was placed on ground with a white paper as background. A uniform background colour allows the use of digital masks so the digitalization can be limited to the sample, facilitating the generation and further edition of the 3D model. Automatic marking of the images was performed by means of ring black coded targets placed on ground. The distances between coded targets were measured with a steel tape and therefore the model was scaled. The photogrammetric network (67 images) consisted in several overlapping parallel and cross lines with oblique photographs and some additional convergent photographs in rough relief areas to avoid hidden areas in the digits (Fig. 3).

In the case of the second group of the Cambil footprints (1B and 2B; Table 1), the samples were surveyed in the field and several rings of images were taken all around the footprints at proper distances. Some coded targets and distances between them were also measured. It is important to mention the high risk of destruction of this outcrop recently discovered in the dump, so the photogrammetric documentation has allowed the virtual conservation of these footprints.

4 Results

4.1 Santisteban del Puerto footprints

A total of 34 footprints were scanned at the 18-m^2 outcrop of Santisteban del Puerto (Fig. 2). Only 17 trace fossils are

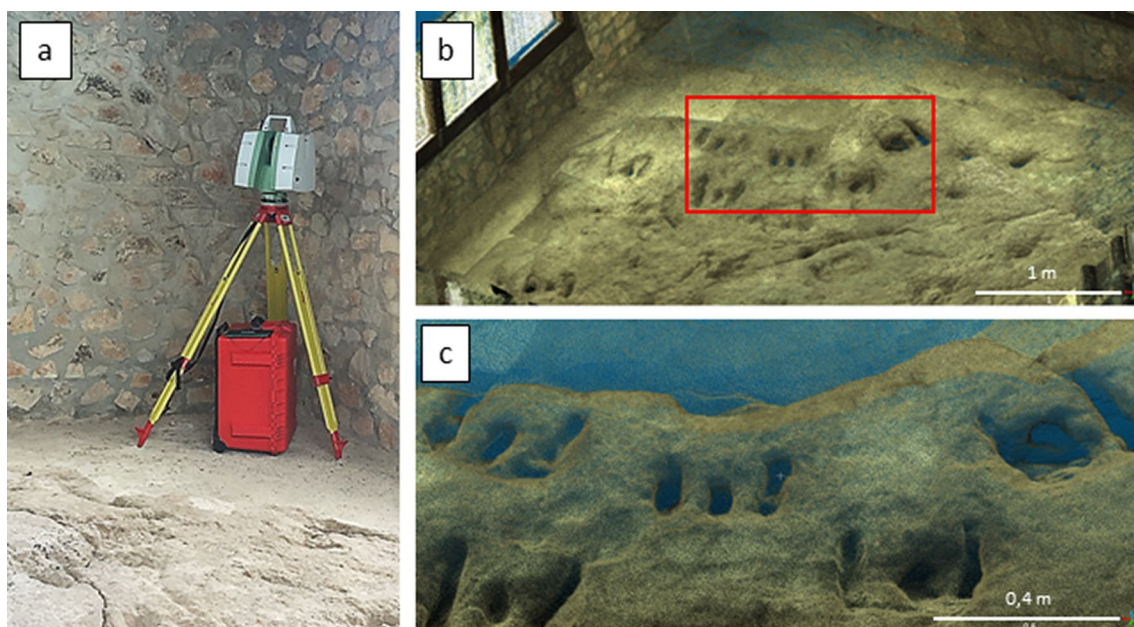
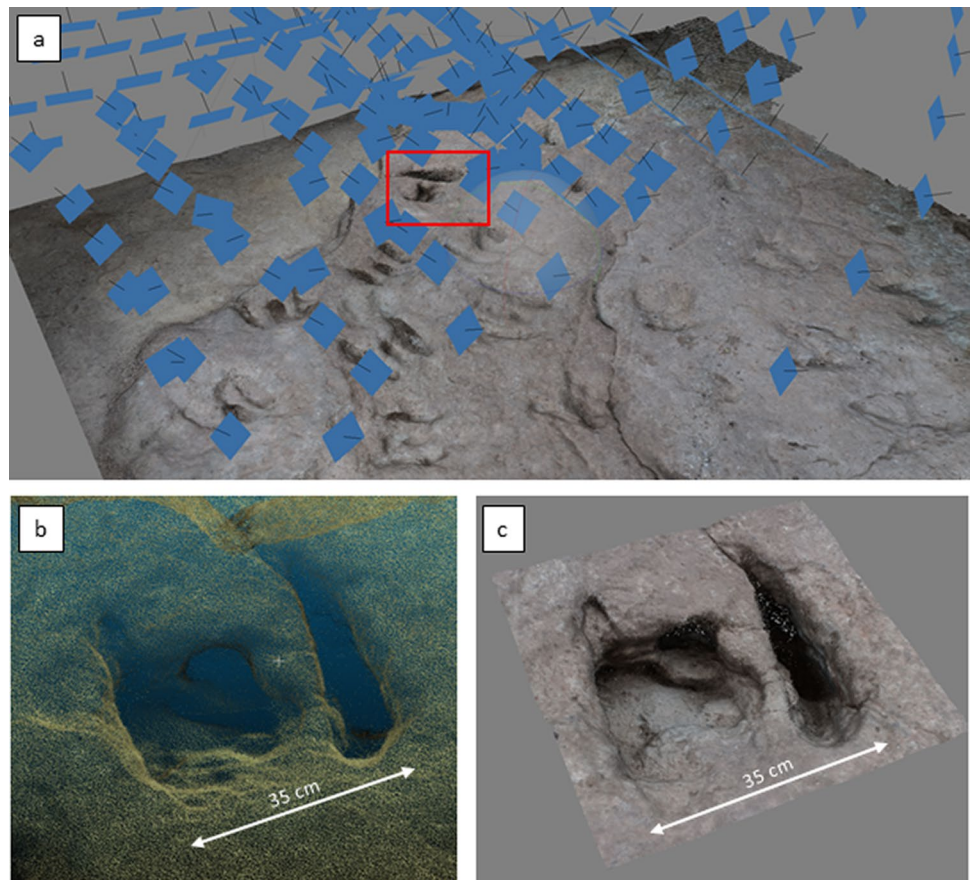


Fig. 4 **a** Leica C10 laser scanner at Santisteban del Puerto outcrop; **b** general view of the laser point cloud; **c** detailed view of the point cloud (red rectangle in 4b), blue areas indicate occluded parts at the footprints where laser cannot measure

Fig. 5 Santisteban del Puerto outcrop. **a** photogrammetric network geometry with 189 oblique parallel and convergent photographs. **b** Laser point cloud section of footprint 4 (red rectangle in **a**), occluded areas where laser cannot measure are visible. **c** merged photogrammetric and laser point cloud of footprint 4, a higher density of point cloud is reached and occluded areas are reduced



well-preserved. Nearly all traces are oriented in the same direction, dominantly N 100°–120° E (Fig. 6). No clear trackways can be identified, and therefore, typical measurements of distances and angles of vertebrate trackways are not available. The total length of the footprints ranges from 28 to 48 cm, and the width from 23 to 44 cm. Each footprint consists of three subparallel concave impressions including two long lateral traces, and a shorter medial one (Fig. 7). The depth of the footprints varies throughout the outcrop (Fig. 6); but commonly the medial trace is the deepest one (Figs. 6, 7).

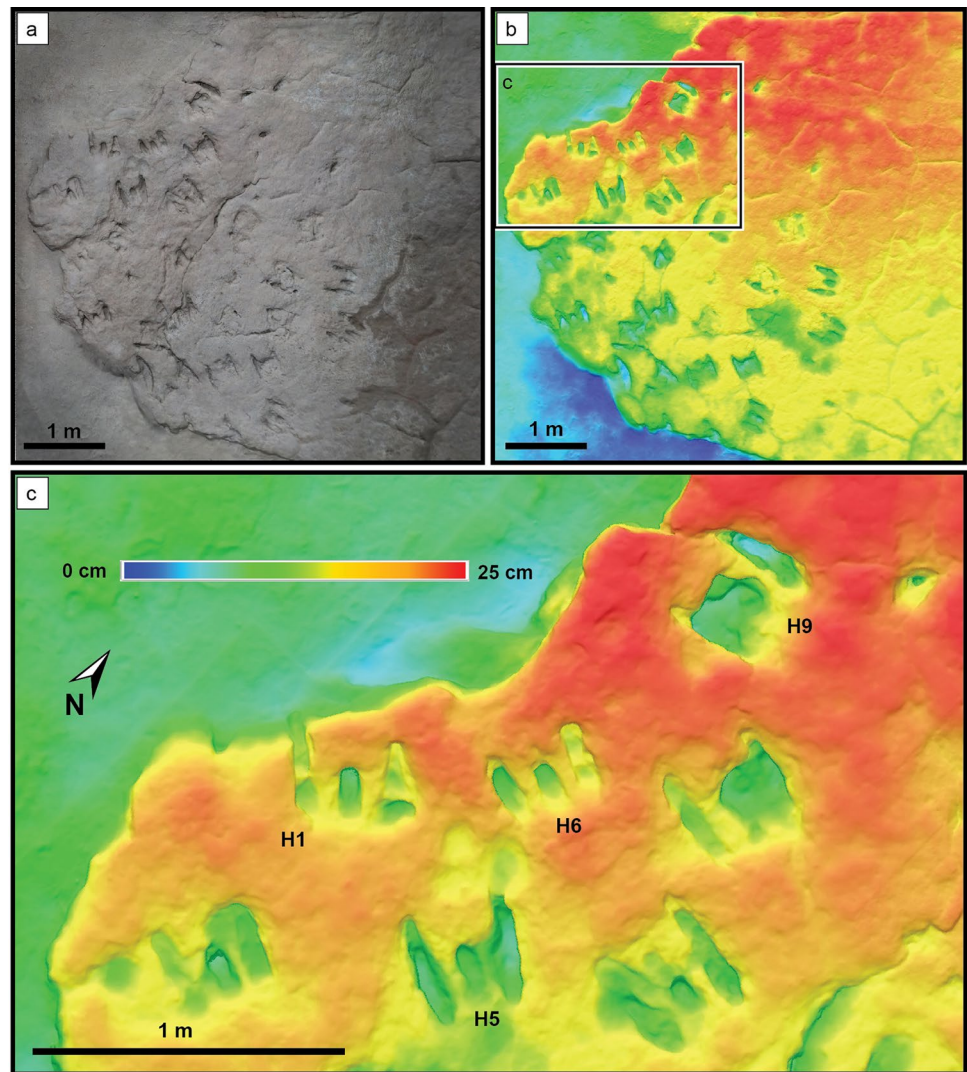
The medial trace is 8–27 cm long from the first contour line at its front to the inner wall of the cavity at its back. The medial trace is commonly located farther back than the others, and presents a clear asymmetry of the trace walls (Fig. 7). Lateral walls are subvertical and have contour lines merging into a single one in plain view (Fig. 6). In contrast, the front of the medial trace shows a gentle slope with ellipsoidal contour lines that are tangent to the back and lateral walls of the trace (Fig. 7). The back wall of the medial trace is sometimes subvertical, but it is commonly not visible due to the cave form of most of the traces (Fig. 7). Three specimens consist exclusively of the medial trace with the characteristic oblique penetration into the sediment.

The external impression length ranges from 21 to 42 cm. In general, the traces become narrower toward their proximal and distal ends (Fig. 7). Sometimes, a sharp-claw impression may be identified at the distal end of the lateral traces. These traces also show a certain asymmetry with subvertical lateral-walls with merging contour lines and gently-inclined proximal and distal ends with well-spaced contour lines (Fig. 7). The overall geometry of the contour lines of the lateral traces consists of a succession of concentric ellipsoids that are tangent to the lateral walls. Sometimes these ellipsoids may be deformed when one of the lateral traces is partially connected to the medial trace (i.e., Fig. 7o).

4.2 Cambil footprints

A total of six footprints from Cambil (Subbetic) were scanned (Fig. 8). Four of them (Pd₁ and Md₁, Pz₂, and Pz₁; Table 1) belong to the trackway composed of eight footprints described by Pérez-López (1993) and have been classified as *Brachychirotherium* (Fig. 9, 10). The other two footprints (1B and 2B, Table 1) were recently discovered in different strata close to the other trackway (Fig. 11). The footprints consist of digitigrade to semi-plantigrade (manus) and semi-plantigrade (pes) impressions preserved as hyporeliefs at the

Fig. 6 Overview of the Santisteban del Puerto outcrops. **a** 3D model with original texture of the outcrop. **b** Digital elevation model of Santisteban del Puerto outcrop. **c** Close-up of the digital elevation model including the footprints displayed in Fig. 7 labelled according to the nomenclature of Reolid and Reolid (2017)



bottom of inverted strata. Pd_1 and Md_1 constitute a manus set (Fig. 9) while the rest of the impressions exclusively are pes imprints (Pz_2 and Pz_1 in Fig. 10, 1B and 2B in Fig. 11). All the footprints have distinct impressions of digits I–IV and partial impressions of digit V. The total length of the footprints ranges from 12 to 30.5 cm, and the width from 15 to 19 cm. The depth of the footprints, or height as they are preserved as moulds, varies throughout the outcrop (Figs. 8, 9, 10, 11).

Only one manus impression, Md_1 , was scanned; it is 14 cm in length and 15 cm in width. The trace displays five short and broad digits and part of the metacarpo-phalangeal area; it is digitigrade to semi-plantigrade. Digits II and III are longest and subequal in length, digits I and IV are shorter, digit V is shortest. The three central digits (II, III, and IV) are well defined, in contrast with the external digits (I and V). The lateral and frontal walls of each digit are subvertical with contour lines merging into a single line (Fig. 9). After digitally inverting the topography of the manus print

mould, the most depressed area of the trace is located in the central part of digits II and III. Also recognizable is the presence of expulsion rims around the manus footprint. It is notable that these rims are higher between digits II and III as well as between digits III and IV, and minor between digits IV and V (Fig. 9).

The rest of the traces are imprints of the hindfeet. The footprints range in size from 30 to 30.5 cm in length and 19 to 20 cm in width. Digit III is longest, followed by digits IV, II and I, which is shortest. The traces are semiplantigrade according to the impressions of part of the metatarsophalangeal portion and digit V (Fig. 9), which is sometimes indistinct (Fig. 11). Digits I–IV are well defined, allowing for measuring their size and interdigital angles (Pérez-López 1993). The walls of the traces are subvertical in their lateral and frontal part, while the back area displays well-spaced contour lines describing a gentle inclination. Some of the digits end with the impression of an up to 2.5-cm-long sharp claw (Fig. 10). In two of the better-preserved footprints,

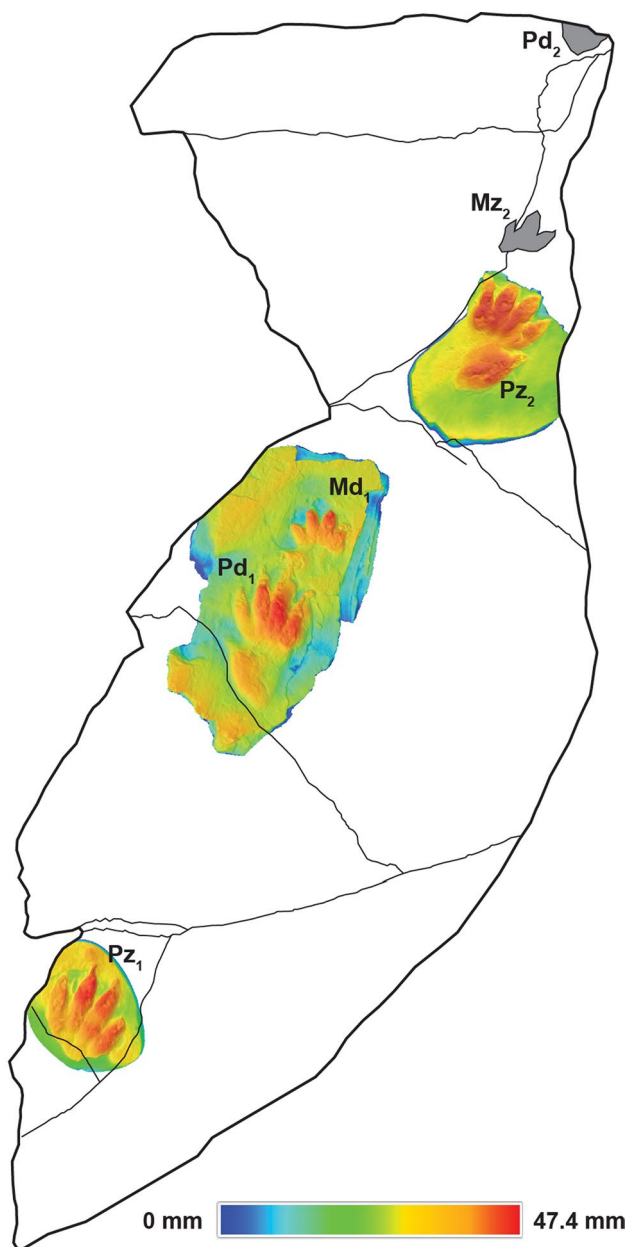


Fig. 7 Detail of some of the footprints of Santisteban del Puerto including from left to right: outcrop close-up, digital elevation model, contour-line map, and 3D view of the subsurface geometry of the footprints. **a–d** Footprint H5 of Reolid and Reolid (2017). Note the angle of separation between the different digits in **d**. **e–h** Footprint H1. **i–l** Footprint H6. **m–p** Footprint H9. Note the claw impressions and the concave upward shape of the footprints H1, H6, and H9 when looking at them from below the surface in **h**, **l**, and **p** respectively

phalangeal and metatarso-phalangeal pads can be distinguished (Figs. 9, 10). The existence of pad impressions is clearly identified in the complex morphology of the contour lines in contrast with the previously-described ellipsoid-shaped ones. The most deeply impressed area of the pes prints corresponds to digits I, II, and III (Figs. 9, 10, 11).

There is a subtle elevation of the substrate near to digits III to IV similar to expulsion rims, but not as obvious as for the manus impressions.

5 Discussion

5.1 Floating-archosaur footprints

The Santisteban del Puerto trace fossils were recently interpreted as the tridactyl footprints of a floating archosaur that only touched the substrate occasionally with the digits II, III, and IV (Reolid and Reolid 2017). The new laser model allows for the validation and refining of this hypothesis. In addition, the previous work of Reolid and Reolid (2017) identified only 26 footprints, but the new treatment of the 3D images and the colour digital elevation model allow the identification of a total of 34 footprints (Fig. 6). The darkest (blue) colour in the digital elevation model indicates the most depressed areas of the traces, these are usually coincident with the medial trace (Fig. 7). The axial digit (III) was probably the longest in the trackmaker's foot and produced the deep medial impression according to Reolid and Reolid (2017). The lateral impressions of the footprints, corresponding to digits II and IV, are in general not as deep as the medial one, and their most depressed areas are located at the central parts of the traces (Fig. 7). According to Reolid and Reolid (2017), the variable depth of the footprints throughout the outcrop is likely related to: (a) a change in the water depth where the archosaurs were floating, (b) differential consistency of the sandy bottom in different parts and time intervals, (c) changes in the sediment grain size and pore-water content of the underlying sandy soft bottom, and (d) differential infill of the footprints by surrounding sediment.

The contour lines in the footprints also indicate peculiarities in the locomotion of the trackmaking archosaur (Mujal et al. 2015). The ellipsoidal contour lines that are tangential to the back and lateral walls of the medial trace indicate that the pressure against the substrate was oblique to the surface. This trajectory of the digits is also evident when the footprints are displaying from below the rock surface (Fig. 7). The 3D visualization allows to rotate the footprints and study them from perspectives that are not physically possible during fieldwork. When visualizing the footprints from below and laterally from the real rock surface it is possible to recognise that the concave upward scratches terminate in a claw impression that it is concave to the top (Fig. 7l). This is consistent with the interpretation of the tip of digit III penetrating into the substrate and being flexed after reaching a certain depth inside the substrate, generating a thixotropic reaction in the underlying sediment. Some of the traces of digits II and IV also record the claw imprint (Fig. 7). When visualizing the part of footprints below the surface from the

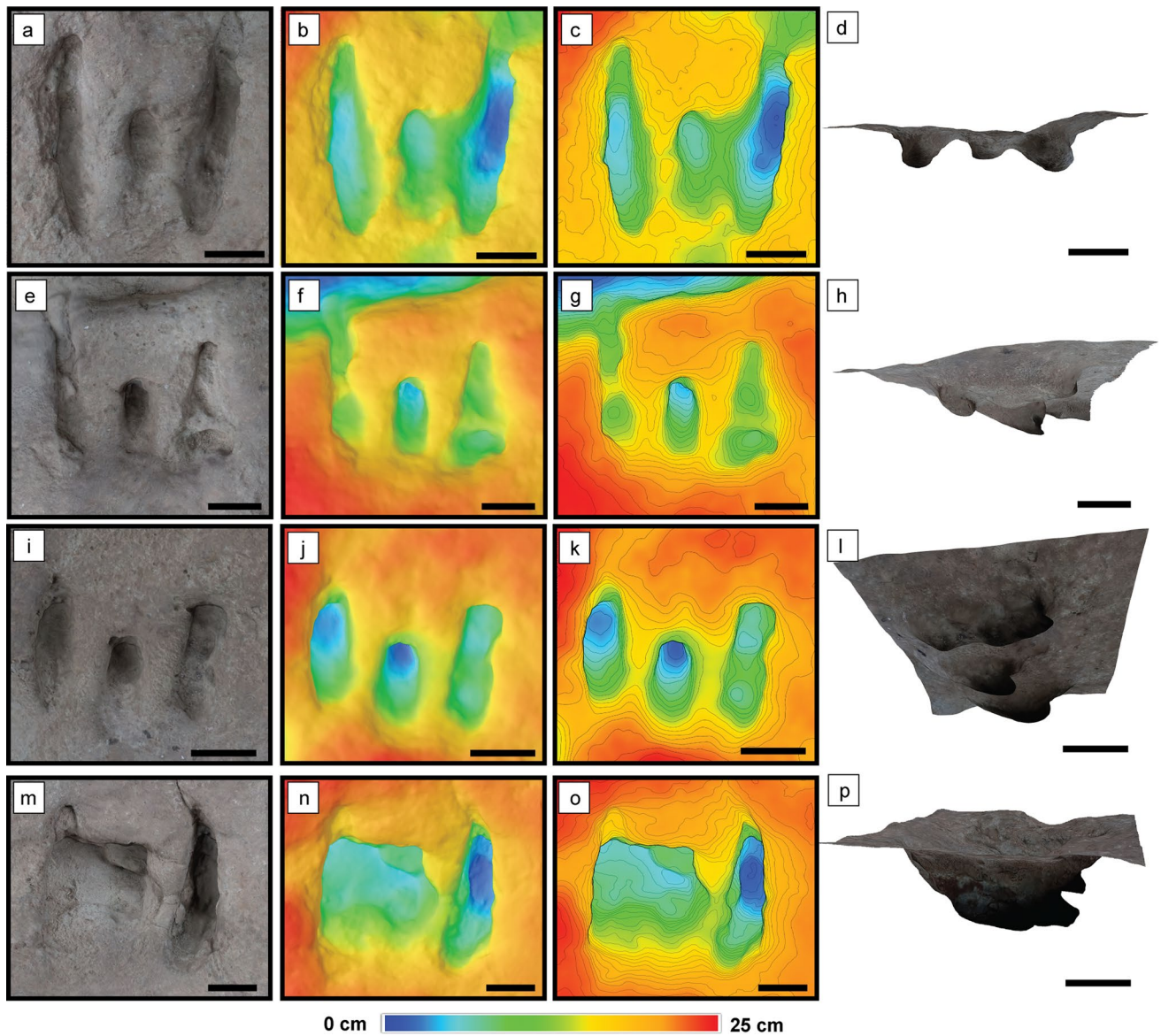


Fig. 8 Representation of the Cambil outcrop using the original diagram and labelling of the footprints of Pérez-López (1993) and superimposed digital elevation model of the footprints

front (Fig. 7d, h), the traces of digit II and IV show the typical divarication between digits as in tracks left by walking archosaurs (i.e., as is the case of the footprints from Cambil outcrop). This is consistent with the interpretation of digits II and IV swinging forward, touching down alongside the anchored axial digit III, and leaving long traces while slipping backward during the kick-off phase (Fig. 12, Reolid and Reolid 2017). In some cases, the most external ellipsoids described by the lateral traces merge with those of the medial trace representing the impression of the joint between digit III and the adjacent digit (Fig. 7g). In summary, the trace fossils of Santisteban del Puerto represents the axial digit of the tracemaker sinking into the sediment and leaving

a short scratch while the lateral traces correspond to the surficial impression of the dorsal surface of the toes and claws. According to Reolid and Reolid (2017), the studied trace fossils correspond to the *Characichnos* ichnofacies, which is swimming tracks composed of parallel scratch marks. The trace maker was a bipedal tridactyl archosaur or some functionally tridactyl chirothere tracemaker. For example, *Poposaurus* developed a dinosaur-like pes (Farlow et al. 2014) and functional analyses of the pelvic and femoral morphology confirm an obligate bipedal gait (Gauthier et al. 2011). Unfortunately, the lack of skeletal remains of the possible tracemakers in the area does not allow for further interpretations.

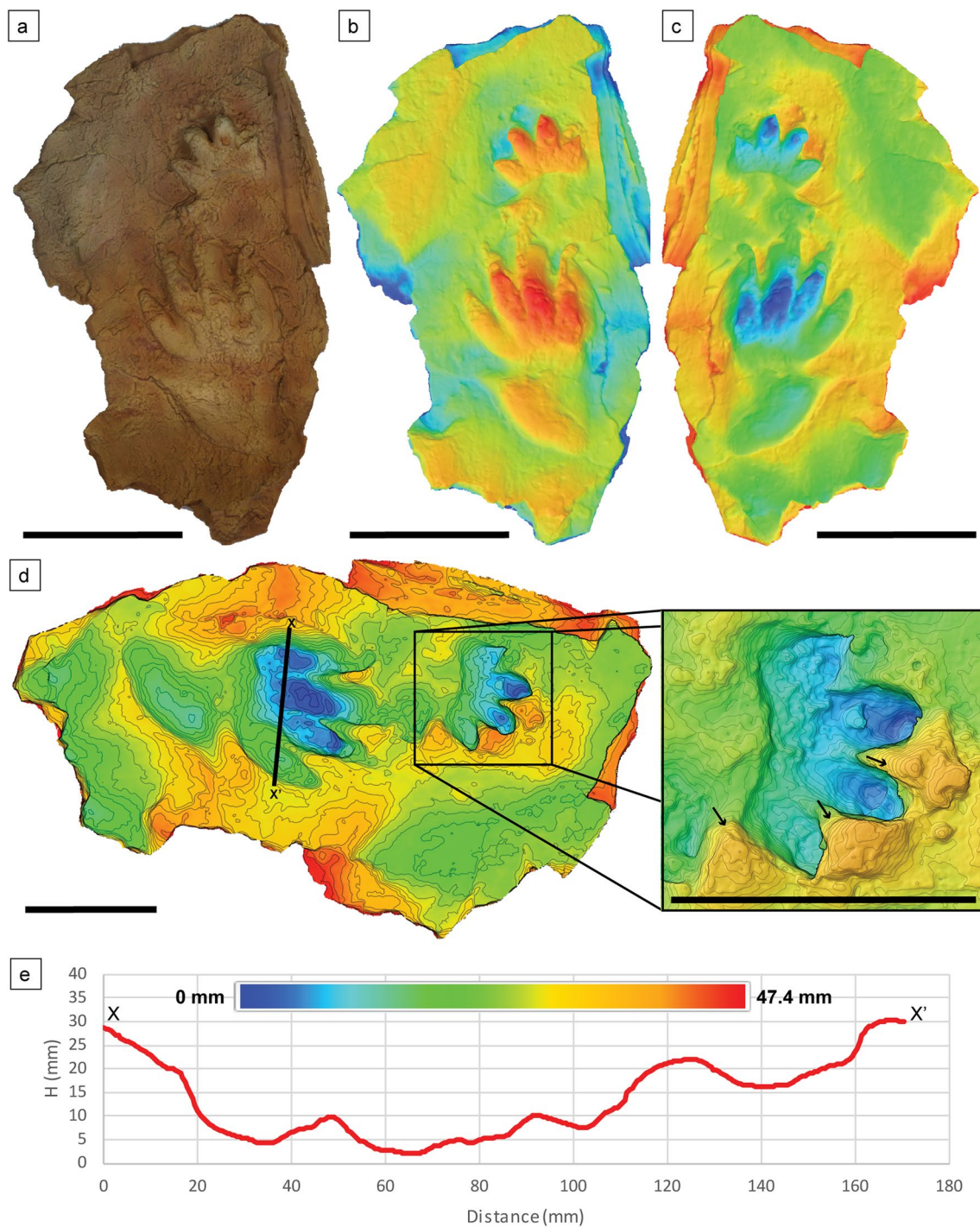


Fig. 9 Detail of the manus-pes set from Cambil (Pd₁ and Md₁ of Pérez-López 1993). **a** 3D model with original. **b** Digital elevation model. **c** Inverted digital elevation model for getting the real foot-

prints instead of the counter mould. **d** Contour-line map and close-up of Md₁. Arrows indicate expulsion rims. **e** Topographic profile of the section marked in the contour-line map

5.2 Walking-archosaur footprints

The footprints of Cambil outcrop are the result of the march of a quadrupedal archosaur, that can be assigned to the ichnofamily Chirotheriidae, probably to *Brachychirotherium*

(Pérez-López 1993) The new methodology allowed the relief inversion for the identification of the areas with greater depth, that is to say, the areas with a higher pressure by the animal during locomotion (Fig. 10, Mujal et al. 2015). The inverted topography shows that the most depressed areas of

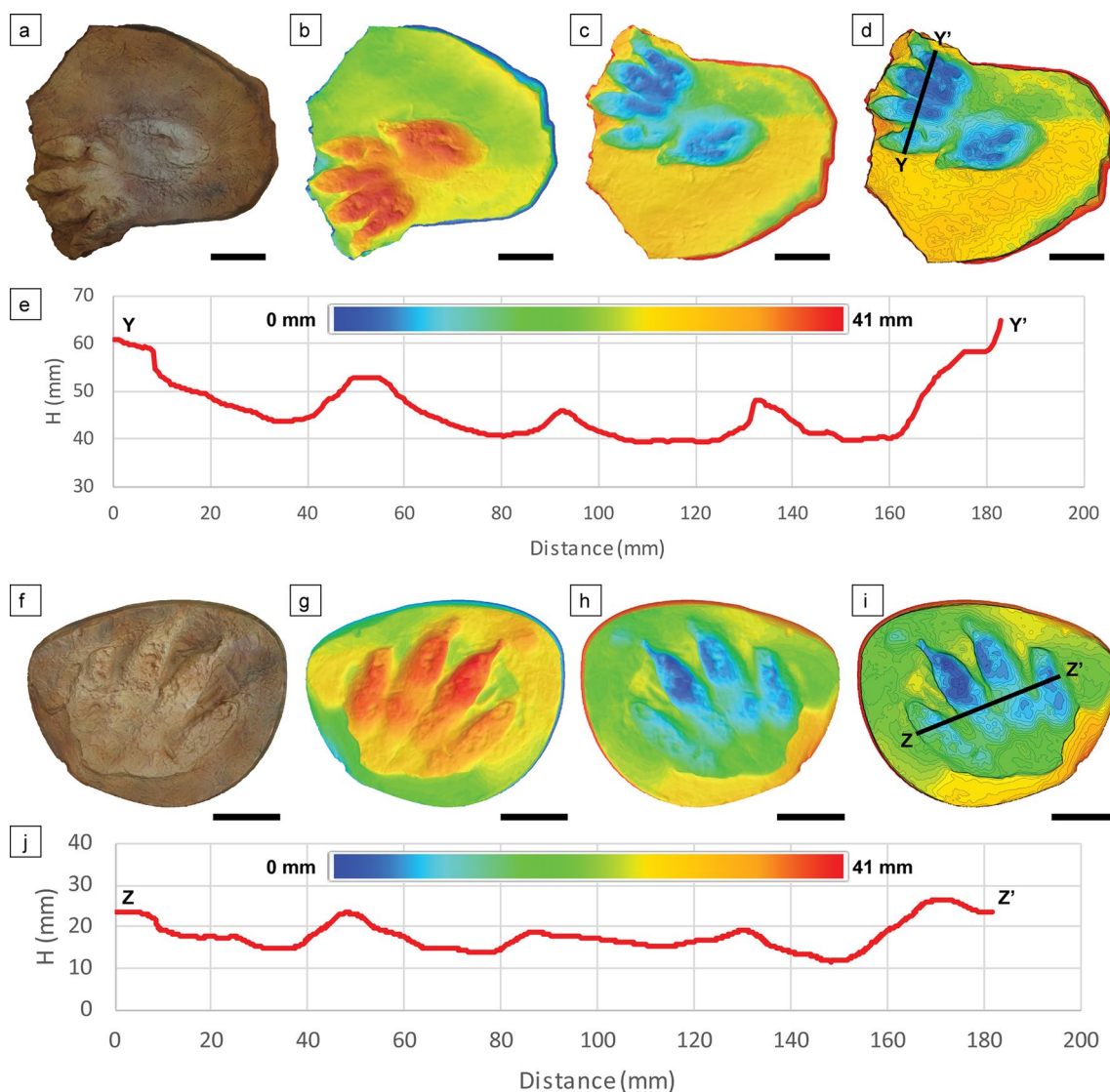


Fig. 10 Detail of the footprints Pz_1 and Pz_2 of Pérez-López (1993), including from left to right outcrop close-up, digital elevation model, inverted digital elevation model for getting the real footprints instead

of the counter mould, contour-line map, and topographic profile of the section marked in the contour-line map. **a–e** Footprint Pz_2 (Table 1). **f–j** Footprint Pz_1 (Table 1)

the traces are located in the central part of digits II and III for the manus imprints, and digits I and II, and minor III, for the pes imprints (Figs. 9, 10, 11).

In the case of the manus, most of the tracemaker's weight laid on the longest digits (II and III). The occurrence of expulsion rims (Fig. 9) was interpreted in similar archosauriform trackways as an indicator of the manus pushing towards the lateral side during impression, generating a higher accumulation of sediment in this direction (Mujal et al. 2017). This, together with the minor impression of digit I supports the interpretation of digitigrade to semi-digitigrade traces of the manus (Pérez-López, 1993; Mujal et al. 2017). This is typical of *Brachychirotherium* traces

elsewhere (Klein and Haubold 2007; Navarro and Moratalla 2018).

In the case of the pes footprints, the digitally-generated depth maps suggest that most of the weight of the animal was load on the internal part of the foot (digits I, II, and III). The pressure distribution estimated out of the trace depth indicates that the tracemaker's forelimbs and hindlimbs performed a pronated walk. This walking behaviour was previously reported from skeletal remains of tetrapods (Hutson 2010, 2014), but here it is first described for *Brachychirotherium* footprints (Fig. 13). According to Klein et al. (2015), the possible tracemaker of *Brachychirotherium* footprints most likely was a stem-crocodylian archosaurs because of the broader configuration of the metatarsals typical of

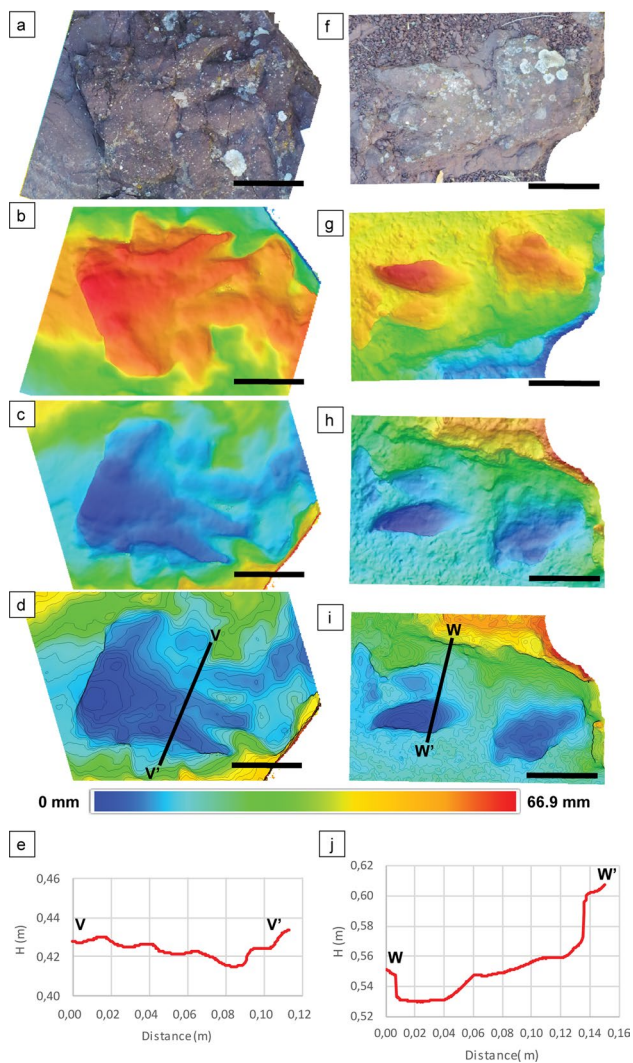


Fig. 11 Detail of the new-discovered footprints of Cambil including from top to bottom outcrop close-up, digital elevation model, inverted digital elevation model for getting the real footprints instead of the counter mould, contour-line map, and topographic profile of the section marked in the contour-line map. **a–e** Footprint 1B (Table 1). **f–j** Footprint 2B (Table 1)

rauisuchians, crocodylomorphs, and aetosaurs (Klein et al. 2006; Nesbitt 2011). The one exception to the broad metatarsals of the stem-crocodylians is the Late Triassic *Poposaurus*, which pes morphology converged with that of the dinosaurs (Farlow et al. 2014). A similar bipedal archosaur could have been the tracemaker of the Santisteban del Puerto footprints (Fig. 12). In summary, the trace fossils of Cambil represent the march of quadruped archosaurs, probably of the ichnogenus *Brachychirotherium*, with pronated digitigrade to semi-plantigrade forelimb-impressions and semi-plantigrade hindlimb impressions (Fig. 13).

5.3 Significance of the vertebrate footprints

The studied outcrops of Cambil (External Subbetic) and Santisteban del Puerto (Tabular Cover) represent the only ichnological record of Triassic terrestrial vertebrates in the southern Iberian Peninsula. In southern Spain, marine vertebrates of the Triassic are relatively common (Niemeyer 2002; Reolid et al. 2014), but evidence of terrestrial fauna is restricted to these two study outcrops from the Tabular Cover and Subbetic. In Europe, ichnological records of terrestrial vertebrates in the Triassic are also documented from central (Navarro and Moratalla 2018) and northern Spain (Gand et al. 2010; Díaz-Martínez and Pérez-García 2012; Díaz-Martínez et al. 2015; Mujal et al. 2017, 2018; Reolid et al. 2018), and from other regions in central and southern Europe, i.e., France (Demathieu 1985), Germany (Klein and Haubold 2007; Diedrich 2012; Klein and Lucas 2018), Switzerland (Avanzini and Cavin 2009; Klein et al. 2016), or Italy (Avanzini and Lockley 2002; Avanzini and Leonardi 2002; Avanzini and Mietto 2008; Santi et al. 2015). However, the Jaén outcrops are the southernmost record of trace fossils of the Triassic in Europe. The study outcrops not only demonstrate the existence of terrestrial tetrapods in this area, they also give new information about the different locomotion styles of Triassic archosaurs including swimming/float-ing of bipeds (Fig. 12) and walking of quadrupeds (Fig. 13).

These trace fossils are of a proven great interest from the scientific point of view but also from the cultural perspective. The scarcity of these kind of outcrops in southern Spain makes the footprints of Jaén a valuable palaeontological heritage. Several actions were carried out by the local authorities and scientists in order to preserve these traces. In the case of Santisteban del Puerto, a small and closed cabin was built to protect the trace fossils from weathering and vandalism. The building allows the observation of the traces through windows and can be visited by making an appointment with the village council. The area is also decorated with some, inaccurate, reconstructions of dinosaurs to enhance the touristic interest of the outcrop. In the case of Cambil, the archosaur footprints were removed from its natural place for their further study and exhibition at the Parque de las Ciencias de Granada, a science museum. The footprints were previously studied at the University of Granada where several replicas of the traces were produced. One of the replicas was displayed in the Centro Paleontológico de Cambil (Cambil Palaeontological Center), together with explanatory panels about the palaeontological and geological heritage in the area. The museum also presents a short movie explaining the formation of the archosaur footprints.

The digitalization of the footprints described in this work is proposed as a useful tool for both the study and the preservation and dissemination of such outcrops. The digitalized data provide information that classical ichnological works

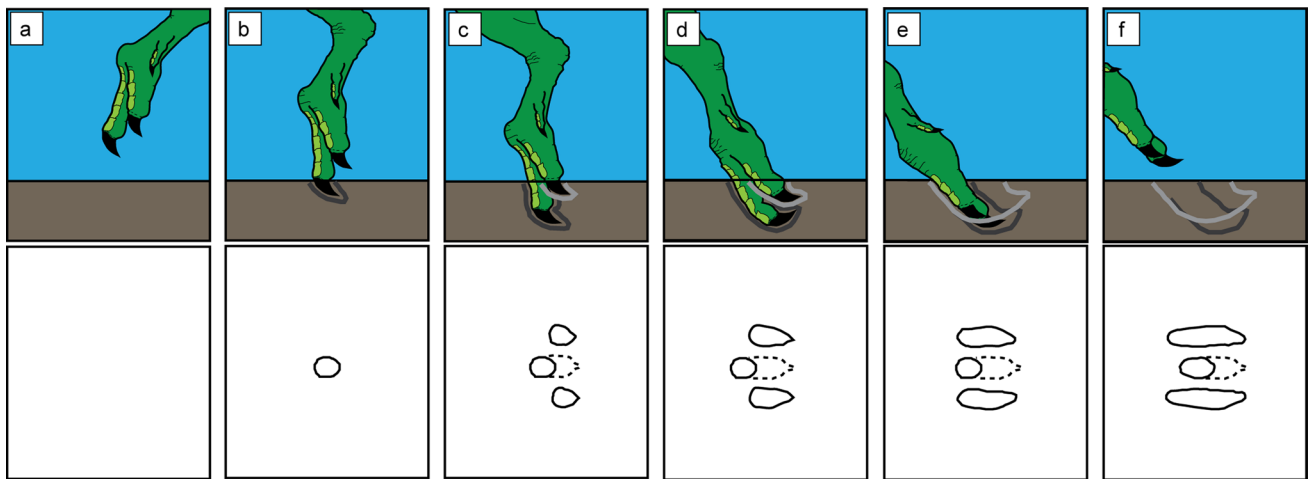


Fig. 12 Reconstruction of different phases of footprint formation during floating of the tracemaker (modified after Reolid and Reolid 2017). Each diagram shows position of the foot in profile (up) and the corresponding plan view of the footprint (down). **a** Foot before touching the bottom. **b** The tip of digit III penetrates the substrate and is anchored in place during the kick-off phase. **c** Kick-off phase con-

tinues and digits II and IV swing forward to touch down alongside the anchored digit III producing claws impressions below the surface. **d** While digit III is anchored the foot rotates producing the concave upward morphology typical of these footprints. **e** Digit III withdraws from the substrate and digits II and IV produce a larger mark by slipping during kick-off phase. **f** The foot exits the substrate

traditionally did not generate. The relief inversion, the depth distribution, the contour line maps, or the topographic profiles of the footprints implement the interpretation obtained during the fieldwork. The digitalization of footprints can also be used as a tool for the preservation and the dissemination of palaeontological outcrops. This modelling and digital representation of reality provides the unquestionable advantage of allowing access to the object in a virtual way, avoiding its manipulation and therefore facilitating its conservation. Among other benefits, important points are the transmission of digital information, the durability over time (digital model), the improvement of the precision in measurements and last but not least, the generation of visually attractive products for its diffusion and use in educational and museum programs (Tejado 2005). This technique allows the visualization of an outcrop without any need of actual visit to the field. This is of great interest because (1) the information recorded in the rock will be accessible even if the outcrop is deteriorated by weathering or human activity; (2) a reduced number of visits to the outcrop will potentially increase its preservation through time; (3) it allows people with limited mobility the access to the palaeontological heritage that otherwise would be only available in outcrops with difficult accessibility.

Photogrammetry and TLS have traditionally been considered as complex and high cost techniques. The need of skilled and experienced personnel and the use of highly sophisticated calibrated instruments and processing systems have prevented the extensive use of Geomatics in Palaeontology, although its utility has by no means been unquestionable (Caracuel et al. 2001, 2002; Cardenal et al. 2001). Nevertheless, at present new methods, instruments

and user-friendly software as those used in this study allow for the effective use of these techniques. Geosciences photogrammetric applications have been stimulated by the improvement of the performance of these systems, the use of conventional non-calibrated (non-metric) off-the-shelf cameras, but also the use of new algorithms in computer vision.

6 Conclusions

The application of 3D photogrammetric models to the analysis of the archosaur (*Pseudosuchia*) footprints from the Middle-Upper Triassic of the south Iberian palaeomargin improved the knowledge and interpretation of the behaviour of archosaurs in this area. A total of 34 footprints were scanned in Santisteban del Puerto (Tabular Cover). Most of the footprints consist of three subparallel concave impressions including two long lateral traces, and a shorter and deeper medial one. In Cambil (Subbetic), a total of six footprints were scanned including 4 out of a trackway composed of 8 footprints and 2 recently discovered ones in the nearby. The footprints are preserved as hyporeliefs at the bottom of inverted strata.

The 3D photogrammetric models allow transformations as the relief inversion and generate new data sets including depth distribution maps, contour line maps, and topographic profiles of the footprints that implement the interpretation obtained during the fieldwork. These are useful tools for the study and the preservation and dissemination of such outcrops. The depth distribution maps indicate the most depressed areas of the traces are usually coincident with the

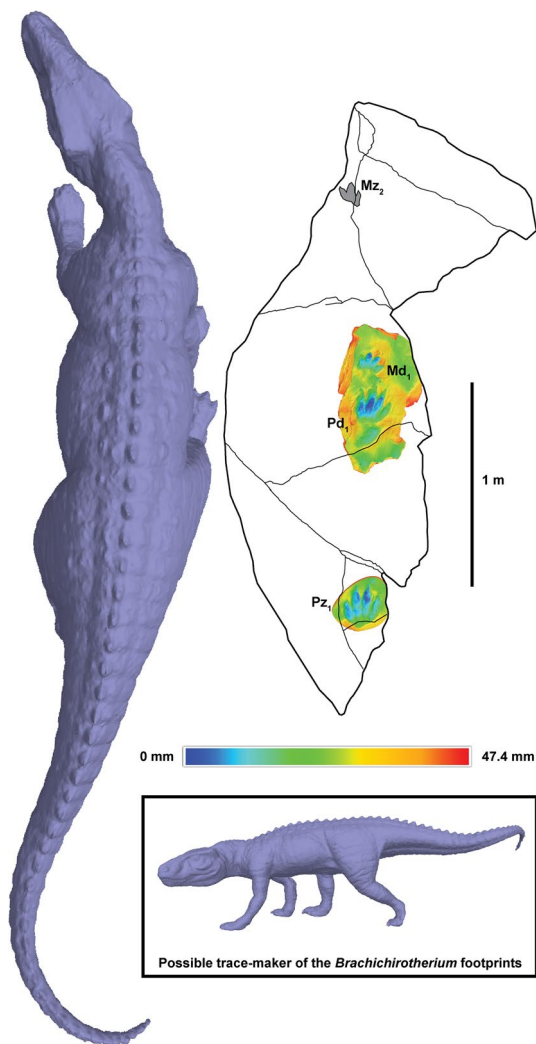


Fig. 13 Plan view of the possible trace-maker of the Cambil footprints at the time of the impressions of Pz₁, Pd₁, Md₁, and Mz₂

medial trace in Santisteban del Puerto and those located in the central part of digits II and III for the manus imprints, and digits I and II, and minor III, for the pes imprints in the ichnogenus *Brachychirotherium* in Cambil. *Brachychirotherium* is interpreted as a quadrupedal rauisuchian archosaur (Clade Rauisuchoidea) with pronated digitigrade forelimb-impressions and semiplantigrade hindlimb impressions. The contour line maps and the 3D rotation of the footprints help in understanding the locomotion of the archosaur. The observed concave-upward claw impressions of Santisteban del Puerto footprints indicate oblique pressure against the substrate by the trace-maker digits. In the case of the Cambil material, the contour lines map indicates that the pressure against the substrate was perpendicular with a slightly oblique component towards the anterior and lateral (outer) side.

The studied outcrops of Cambil (External Subbetic) and Santisteban del Puerto (Tabular Cover) represent the only ichnological record of Triassic terrestrial vertebrates in the southern Iberian Peninsula, and the southernmost record of trace fossils of the Triassic in Europe. The study outcrops document the existence of terrestrial tetrapods and provide information about the different locomotion styles of Triassic rauisuchian archosaurs including swimming/floating bipedal individuals (probably *Poposauroidea*) and walking quadrupeds (*Rauisuchoidea*).

Acknowledgements JR research was supported by the Juan de la Cierva Program (Ministerio de Ciencia, Innovación y Universidades). JR is also thankful for funding from research group RNM-190 (Junta de Andalucía). FJC and MR want to thank funding by Project PALEOV-UJA (Instituto de Estudios Giennenses, IEG2018). All authors thank the valuable comments of associate editor Laura Domingo, reviewer Hendrik Klein, and an anonymous reviewer that improved the final version of this manuscript.


References

- AGISOFT. (2019). Agisoft PhotoScan: <https://www.agisoft.com/>. Accessed March 2019.
- Avanzini, M., & Cavin, L. (2009). A new *Isochirotherium* trackway from the Triassic of Vieux Emosson, SW Switzerland: Stratigraphic implications. *Swiss Journal of Geosciences*, *102*, 353–361.
- Avanzini, M., & Leonardi, N. (2002). *Isochirotherium inferni* ichnosp. Nov. In the Illyrian (Late Anisian, Middle Triassic) of Adige Valley (Bolzano, Italy). *Bolletino Societa Paleontologica Italiana*, *41*, 41–50.
- Avanzini, M., & Lockley, M. (2002). Middle Triassic archosaur population structure: Interpretation based on *Isochirotherium delicatum* fossil footprints (Southern Alps, Italy). *Palaeogeography, Palaeoclimatology, Palaeoecology*, *185*, 391–402.
- Avanzini, M., & Mietto, P. (2008). Lower and Middle Triassic footprint-based Biochronology in the Italian Southern Alps. *Oryctos*, *8*, 3–13.
- Bourquin, S., Bercovici, A., López-Gómez, J., Diez, J. B., Broutin, J., Ronchi, A., et al. (2011). The Permian-Triassic transition and the onset of Mesozoic sedimentation at the northwestern peri-Tethyan domain scale: Palaeogeographic maps and geodynamic implications. *Palaeogeography, Palaeoclimatology, Palaeoecology*, *299*, 265–280.
- Brusatte, S. L., Benton, M. J., Desojo, J. B., & Langer, M. C. (2010). The higher-level phylogeny of Archosauria (Tetrapoda: Diapsida). *Journal of Systematic Palaeontology*, *8*, 3–47.
- Caracuel, J., Cardenal, J., & Delgado, J. (2002). Aplicaciones fotogramétricas digitales en el análisis morfométrico de fósiles. *Boletín Geológico y Minero*, *113*, 85–95.
- Caracuel, J., Cardenal, J., Delgado, J., & Boix, M. (2001). Modelización digital de macroinvertebrados fósiles con escáner 3D. In *XVII Jornadas de la SEP: los fósiles y la paleogeografía*. *Pub. Sepaz*, *5.2* (pp. 637–642).
- Cardenal, J., Delgado, J., Caracuel, J. E., & Ordoño, L. (2001). Sistemas fotogramétricos automatizados para la obtención de medidas y visualización de grandes restos fósiles. In *XVII Jornadas de la SEP: los fósiles y la paleogeografía*. *Pub. Sepaz*, *5.2* (pp. 643–648).

- CloudCompare (version 2.6.3) [GPL software]. (2019). <https://www.cloudcompare.org/>. Accessed June 2019.
- Cunningham, J. A., Rahman, I. A., Lautenschlager, S., Rayfield, E. J., & Donoghue, P. C. J. (2014). A virtual world of paleontology. *Trends in Ecology & Evolution*, 29(6), 347–357.
- Demathieu, G. (1985). Trace fossil assemblages in Middle Triassic marginal marine deposits, eastern border of the Massif Central, France. *SEPM Special Publication*, 35, 53–66.
- Demathieu, G., & Demathieu, P. (2004). Chirotheria and other ichnotaxa of the European Triassic. *Ichnos*, 11, 79–88.
- Demathieu, G. R., Pérez-López, A., & Pérez-Lorente, F. (1999). Enigmatic ichnites in the middle Triassic of Southern Spain. *Ichnos*, 6, 229–237.
- Demathieu, G., Ramos, A., & Sopena, A. (1978). Fauna icnológica del Triásico del extremo noroccidental de la Cordillera Ibérica (Prov. de Guadalajara). *Estudios Geológicos*, 34, 175–186.
- Díaz-Martínez, I., Castanera, D., Gasca, J. M., & Canudo, J. I. (2015). A reappraisal of the Middle Triassic chirotherid *Chirotherium ibericus* Navás, 1906 (Iberian Range, NE Spain), with comments on the Triassic tetrapod track biochronology of the Iberian Peninsula. *Peer J*, 3, e1044.
- Díaz-Martínez, I., & Pérez-García, A. (2012). Historical and comparative study of the first Spanish vertebrate paleoichnological record and bibliographic review of the Spanish chirotheriid footprints. *Ichnos*, 19, 141–149.
- Diedrich, C. G. (2012). Middle Triassic chirotherid trackways on earthquake influenced intertidal limulid reproduction flats of the European Germanic Basin coasts. *Central European Journal of Geosciences*, 4, 495–529.
- Evin, A., Souter, T., Hulme-Beaman, A., Ameen, C., Allen, R., Viacava, P., et al. (2016). The use of close-range photogrammetry in zooarchaeology: Creating accurate 3D models of wolf crania to study dog domestication. *Journal of Archaeological Science: Reports*, 9, 87–93.
- Farlow, J. O., Schachner, E. R., Sarrazin, J. C., Klein, H., & Currie, P. J. (2014). Pedal proportions of *Poposaurus gracilis*: Convergent and divergent in the feet of archosaurs. *The Anatomical Record*, 297, 1022–1046.
- Fernández, J. (1977). *Sedimentación triásica en el borde SE de la Meseta*. Unpublished Ph.D. Thesis, Universidad de Granada, Granada, Spain.
- Fortuny, J., Bolet, A., Selles, A. G., Cartanya, J., & Galobart, A. (2011). New insights on the Permian and Triassic vertebrates from the Iberian Peninsula with emphasis on the Pyrenean and Catalan basins. *Journal of Iberian Geology*, 37, 65–86.
- Gand, G., De La Horra, R., Galán-Abellán, B., López-Gómez, J., Barrenechea, J. F., Arche, A., et al. (2010). New ichnites from the Middle Triassic of the Iberian Ranges (Spain): Paleoenvironmental and paleogeographical implications. *Historical Biology*, 22, 40–56.
- Gauthier, J. A., Nesbitt, S. J., Schachner, E. R., Bever, G. S., & Joyce, W. G. (2011). The bipedal stem crocodylian *Poposaurus gracilis*: Inferring function in fossils and innovation in archosaur locomotion. *Bulletin of the Peabody Museum of Natural History*, 52, 107–126.
- Haubold, H. (1971). Die Tetrapodenfährten des Buntsandsteins. *Paläontologische Abhandlungen*, IV (pp. 395–548)
- Hutson, J. D. (2010) *A Functional Study of the Origins of Tetrapod Forelimb Pronation*. M.Sc. Thesis, Northern Illinois University, DeKalb, Illinois, USA. <https://gradworks.umi.com/1480796.pdf>.
- Hutson, J. D. (2014). Quadrupedal Dinosaurs did not evolve fully pronated forearms: New EVIDENCE from the Ulna. *Acta Palaeontologica Polonica*, 60(3), 599–610.
- Klein, H., & Haubold, H. (2007). Archosaur footprints: Potential for biochronology of Triassic continental sequences. *New Mexico Museum of Natural History and Science Bulletin*, 41, 120–130.
- Klein, H., & Lucas, S. G. (2018). Diverse Middle Triassic tetrapod footprints assemblage from the Muschelkalk of Germany. *Ichnos*, 25, 162–176.
- Klein, H., Lucas, S. G., & Haubold, H. (2006). Tetrapod track assemblage of the Redonda Formation (Upper Triassic, Chinle Group) in east-central New Mexico—Reevaluation of ichnofaunal diversity from studies of new material. *New Mexico Museum of Natural History and Science Bulletin*, 37, 241250.
- Klein, H., Milàn, J., Clemmensen, L. B., Frobøse, N., Mateus, O., Klein, N., et al. (2015). Archosaur footprints (cf. Brachychirotherium) with unusual morphology from the Upper Triassic Fleming Fjord Formation (Norian–Rhaetian) of East Greenland. *Geological Society of London, Special Publications*, 434, 71–85.
- Klein, H., Wizevich, M. C., Thürring, B., Marty, D., Thürring, S., Falkingham, P., et al. (2016). Triassic chirotheriid footprints from the Swiss Alps: Ichnotaxonomy and depositional environment (Cantons Wallis & Glarus). *Swiss Journal of Palaeontology*, 135, 295–314.
- Lagnaoui, A., Melchor, R. N., Bellosi, E. S., Villegas, P. M., Espinoza, N., & Umazano, A. M. (2019). Middle Triassic *Pentasauropus*-dominated ichnofauna from western Gondwana: Ichnotaxonomy, palaeoenvironment, biostratigraphy and palaeobiogeography. *Palaeogeography, Palaeoclimatology, Palaeoecology*, 524, 41–61.
- López-Garrido, A. C. (1971). *Geología de la zona Prebética, al NE de la provincia de Jaén*. Ph.D. Thesis, Universidad de Granada, Granada, Spain.
- López-Gómez, J., Galán-Abellán, B., de la Horra, R., Barrenechea, J. F., Arche, A., Bourquin, S., et al. (2012). Sedimentary evolution of the continental Early-Middle Triassic Canizar Formation (Central Spain): Implications for life recovery after the Permian-Triassic crisis. *Sedimentary Geology*, 249, 26–44.
- Mallison, H., & Wings, O. (2014). Photogrammetry in paleontology: A practical guide. *Journal of Paleontological Techniques*, 12, 1–31.
- Marchetti, L., Klein, H., Buchwitz, M., Ronchi, A., Smith, R. M. H., de Klerk, W. J., et al. (2019). Permian-Triassic vertebrate footprints from South Africa: Ichnotaxonomy, producers and biostratigraphy through two major faunal crises. *Gondwana Research*, 72, 139–168.
- Molnar, J. L., Pierce, S. E., Clack, J. A., & Hutchinson, J. R. (2012). Idealized landmark-based geometric reconstructions of poorly preserved fossil material: A case study of an early tetrapod vertebra. *Palaeontologia Electronica*, 15(1), 2T.
- Mujal, E., Fortuny, J., Bolet, A., Oms, O., & López, J. A. (2017). An archosauromorph dominated ichnoassemblage in fluvial settings from the late Early Triassic of the Catalan Pyrenees (NE Iberian Peninsula). *PLoS One*, 12, 0174693.
- Mujal, E., Fortuny, J., Rodríguez-Salgado, P., Diviu, M., Oms, O., & Galobart, A. (2015). First footprints occurrence from the Muschelkalk detrital unit of the Catalan Basin: 3D analyses and palaeoichnological implications. *Spanish Journal of Palaeontology*, 30, 97–108.
- Mujal, E., Gretter, N., Ronchi, A., López-Gómez, J., Falconnet, J., Diez, R. D., et al. (2016). Constraining the Permian/Triassic transition in continental environments: Stratigraphic and paleontological record from the Catalan Pyrenees (NE Iberian Peninsula). *Palaeogeography, Palaeoclimatology, Palaeoecology*, 445, 18–37.
- Mujal, E., Iglesias, I., Oms, O., Fortuny, J., Bolet, A., & Méndez, J. M. (2018). *Rhynchosauroides* footprint variability in a Muschelkalk detrital interval (late Anisian–middle Ladinian) from the Catalan Basin (NE Iberian Peninsula). *Ichnos*, 25(2), 150–161.
- Navarro, O., & Moratalla, J. J. (2018). Swimming reptile prints from the Keuper facies (Carnian, Upper Triassic) of Los Gallegos new tracksite (Iberian Range, Valencia province, Spain). *Journal of Iberian Geology*, 44, 479–496.

- Nesbitt, S. J. (2011). The early evolution of archosaurs: Relationships and the origin of clades. *Bulletin of the American Museum of Natural History*, 398, 1–126.
- Niemeyer, J. (2002). Invertebraten und Vertebraten aus dem Muschelkalk von Siles (Jaén), Spanien. *Münstersche forschungen zur Geologie und Paläontologie*, 94, 1–99.
- Pérez-López, A. (1993). Estudio de las huellas de reptil, del ichnogénero *Brachychiroterium*, encontradas en el Trías subbético de Cambil. *Estudios Geológicos*, 49, 77–86.
- Pérez-López, A. (1998). Epicontinental Triassic of the Southern Iberian continental margin (Betic Cordillera, Spain). In Bachmann, G. H., Lerche, I. (Eds.), *Stuttgart, Epicontinental Triassic, vol. 2. Zentralblatt für Geologie und Paläontologie Teil I* (Heft 9–10, pp. 1009–1031). ISBN 3-510-66014-5.
- Pérez-López, A., & Pérez-Valera, F. (2007). Palaeogeography, facies and nomenclature of the Triassic units in the different domains of the Betic Cordillera (S Spain). *Palaeogeography, Palaeoclimatology, Palaeoecology*, 254, 606–626.
- QGIS Development Team. (2019). *QGIS Geographic Information System*. Open Source Geospatial Foundation. URL <https://qgis.org>. Accessed June 2019.
- Reolid, J., & Reolid, M. (2017). Traces of floating archosaurs: An interpretation of the enigmatic trace-fossils from the Triassic of the Tabular Cover of Southern Spain. *Ichnos*, 24, 222–233.
- Reolid, M., Márquez-Aliaga, A., Belinchón, M., García-Fórner, A., Villena, J., & Martínez-Pérez, C. (2018). Ichological evidence of semi-aquatic locomotion in early turtles from Eastern Iberia during the Carnian Humid Episode (Late Triassic). *Palaeogeography, Palaeoclimatology, Palaeoecology*, 490, 450–461.
- Reolid, M., Pérez-Valera, F., Benton, M. J., & Reolid, J. (2014). Marine flooding event in continental Triassic facies identified by a nothosaur and placodont bonebed (South Iberian Palaeomargin). *Facies*, 60, 277–293.
- Santi, G., Lualdi, A., Decarlis, A., Nicosia, U., & Ronchi, A. (2015). Chirotheriid footprints from the Lower-Middle Triassic of the Briançonnais Domain (Pelite di Case Valmarecca, Western Liguria, NW Italy). *Bollettino della Società Paleontologica Italiana*, 54, 81–90.
- Simon, O. J. (1987). On the Triassic of the Betic Cordilleras (SE Spain). *Cuadernos de geología ibérica*, 11, 385–402.
- Tejado, J. M. (2005). Escaneado en 3D y prototipado de piezas arqueológicas: Las Nuevas Tecnologías en el registro, conservación y difusión del Patrimonio Arqueológico. *Iberia*, 8(2005), 135–158.
- Zhilin, C., & Baltsavias, E. (2008). *Advances in photogrammetry, remote sensing and spatial information sciences. 2008 ISPRS Congress book*. Boca Raton: CRC Press.

Affiliations

Jesús Reolid¹  · F. Javier Cardenal² · Matías Reolid³ · Emilio Mata²

¹ Departamento de Estratigrafía y Paleontología, Universidad de Granada, Avd. De La Fuente Nueva S/N, 18071 Granada, Spain

² Departamento de Ingeniería Cartográfica, Geodésica y Fotogrametría, Universidad de Jaén, Campus Las Lagunillas sn, 23071 Jaén, Spain

³ Departamento de Geología, Universidad de Jaén, Campus Las Lagunillas sn, 23071 Jaén, Spain